Journal of the Meteorological Society of Japan, Vol. 88, No. 1, pp. 79–90, 2010.
DOI:10.2151/jmsj.2010-106

A Peculiar Feature of the Seasonal Migration of the South American Rain Band

Youichi TANIMOTO and Takushi KAJITANI[1]

Faculty of Environmental Earth Science and Graduate School of Environmental Science, Hokkaido University, Sapporo, Japan

Hideki OKAJIMA

Research Institute for Global Change, Japan Agency for Marine-Earth Science and Technology, Yokohama, Japan

and

Shang-Ping XIE

International Pacific Research Center and Department of Meteorology, University of Hawaii, Honolulu, USA

(Manuscript received 14 April 2009, in final form 28 October 2009)

Abstract

Seasonal migration of tropical rainfall is examined in the South American sector and compared with that over Africa, using satellite and reanalysis data. While the African rain band moves continuously back and forth across the equator following the seasonal march of the sun, the South American one displays a peculiar asymmetry between its northward and southward migration. The rain band moves gradually northward from October to July from the Amazon toward the Caribbean Sea, while its return to the Amazon is an abrupt event, with convection developing rapidly in October around 10°S without going through the equator. Over the equatorial Amazon during July–October, equivalent potential temperature (θ_e) is kept low by the easterly advection of low temperature and humidity air from the equatorial Atlantic, coinciding with the seasonal development of ocean upwelling and a cold tongue in sea surface temperature. The low θ_e values prevent convection from developing in the equatorial Amazon while warm SST supports convection on the north coast of South America during August–October. Meanwhile solar radiation continues to heat up the land surface to the south, eventually triggering the onset of deep convection there in October.

Atmospheric general circulation model experiments were conducted to examine the effect of the Atlantic cold tongue on tropical rain bands. Without the seasonal development of the Atlantic cold tongue, surface θ_e remains high in September, and rainfall in the equatorial Amazon switches to a pronounced semi-annual cycle with a peak in each equinox. These results illustrate the role of the Atlantic cold tongue in the peculiar meridional migration of the observed South American rain band.

1. Introduction

Seasonal migration of tropical rainfall in the meridional direction displays different characteristics over the ocean and land in the hemisphere of 140°W–40°E (Mitchell and Wallace 1992). In this West Hemisphere including the eastern Pacific and Atlantic, the oceanic intertropical convergence zone (ITCZ) is locked onto the meridional maximum of sea surface temperature (SST), both displaced north of the equator. Only during a brief period of March–April, SST south of the equator rises to high enough values for convection. In re-

Corresponding author: Youichi Tanimoto, Faculty of Environmental Earth Science, Hokkaido University, N10 W5, Kita-ku, Sapporo 060-0810, Japan.
E-mail: tanimoto@ees.hokudai.ac.jp
1 Present affiliation: Shimanto City Office

sponse to the seasonal SST warming in the Southern Hemisphere, a double ITCZ astride the equator develops in the eastern Pacific (Waliser and Gautier 1993; Lietzke et al. 2001), while the Atlantic ITCZ reaches its southernmost location and in the western basin, connects with the rain band on northeast South America (Mitchell and Wallace 1992). The development of the climatic asymmetry over the eastern Pacific and Atlantic is a result of ocean-atmosphere interactions triggered by latitudinal asymmetry in continental geometry (Xie and Philander 1994).

Over continents, by contrast, tropical rain bands tend to follow the seasonal march of the sun because of the small heat capacity of soil layers involved in the seasonal cycle. Combining observations over the American and African continents, Mitchell and Wallace (1992) show that deep convection over land moves back and forth across the equator between 15° north and south. This equatorially symmetric migration of the continental ITCZ is confirmed by more recent observations based on a combined satellite-rain gauge data set (Kodama and Tamaoki 2002). This symmetric meridional movement of the rain band is pronounced only in the tropical ITCZ within 25°N/S, but not associated with other rain bands such as the South Pacific and South Atlantic convergence zones (Kodama 1992, 1993).

South America and Africa feature very different geometries. In 10–30°E, the African Continent occupies the entire tropics on both sides of the equator, allowing the rain band to move across the equator in this land strip. The South American Continent, on the other hand, faces the Atlantic Ocean to its north. Because of large differences in heat capacity between South America and the ocean to its north, the meridional migration of the tropical rain band may differ between South America and Africa. Indeed, based on *in-situ* rain gauge and OLR data sets, previous studies (Horel et al. 1989; Marengo et al. 2001; and references therein) pointed out a rapid southward migration during August–October before the onset of the rainy season in the central Amazon, while a northward migration of the rain band is gradual during February–April. Though some discrepancies between *in-situ* and OLR data in location and intensity of the tropical rain band are reported as in Marengo et al. (2001), we confirm this peculiar movement of the rain band over the South America by using new satellite observations and by contrasting these continents that face each other across the Atlantic Ocean. Rainfall in the South American sector displays highly asymmetric migration across the equator, moving gradually from the continent toward the North Atlantic Ocean but featuring a discontinuous jump in the other direction (Fig. 1a).

As a mechanism for an abrupt onset of the rainy season in the Amazon during austral summer (November–January), Williams and Renno (1993) and Fu et al. (1999) showed, based on the *in-situ* soundings, that a local increase of equivalent potential temperature (θ_e) in the planetary boundary layer (PBL) is necessary for the seasonal onset of convection. As stated in Fu et al. (1999), increases

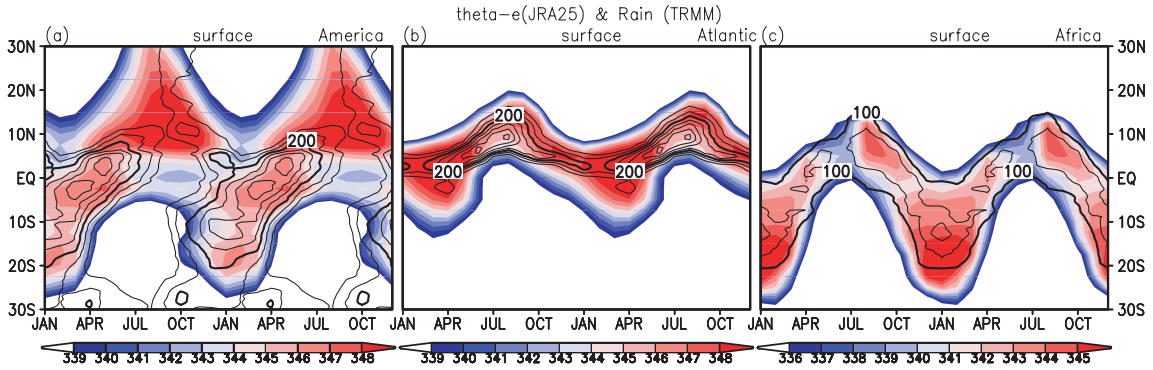

Fig. 1. Latitude-time sections of rainfall (contour at 50 mm month^{-1} intervals) based on the TRMM 3B43 product and JRA-25 equivalent potential temperature at the surface (colors in K) in (a) the South American (60–50°W), (b) Atlantic (20–10°W), and (c) African (20–30°E) sectors. Note that two annual cycles are presented. The longitudinal bands are chosen to avoid high orography of the Andes and African Rift Valley. The Atlantic (African) sector is all ocean (land).

of land surface temperature alone cannot initiate the convection, unlike the increases in SST over the ocean. Given lack of soil moisture before the onset, the small heat capacity of land surface enhances land surface warming, but cannot increase moist static energy near the surface, probably due to insufficient moisture supply from the surface. Fu et al. (1999) suggested that changes in large-scale atmospheric circulation are responsible for increased θ_e in the PBL by moisture transport into the southern Amazon before the onset, while local latent and sensible heat fluxes play minor roles in moistening the lower atmosphere. Wang and Fu (2002) showed that intraseasonal northerly winds in the lower atmosphere intermittently transport moisture into the southern Amazon before the onset. Meanwhile, Fu et al. (1999) suggested that the surface heat fluxes are indirectly responsible for the onset by forming strong land-sea contrast in the lower atmosphere that drives large-scale surface flow toward land. Indeed, Fu and Li (2004) and Li and Fu (2004) showed, based on reanalysis data, that surface heat fluxes over the Amazon begin to increase about 2 months before the large-scale northerly winds initiate the transition from the dry to wet season. They also showed, even before the wet season (rain rate > 8 mm day^{-1}), that the latent heat flux (80–100 W m^{-2}) is larger than sensible heat flux (30–40 W m^{-2}) because of weak rainfall ($\sim$3 mm day^{-1}) in the Amazon. Several studies pointed out that intense subtropical rainfall east of the Andes is provided by the passage of several synoptic frontal systems before its onset (Garreaud and Wallace 1998; Li and Fu 2006; Raia and Cavalcanti 2008), accompanied by intrusions of the extratropical cold air. Over the subtropical South America, the cold air intrusion in the entire troposphere tends to increase relative humidity and the buoyancy in the lower troposphere, and the associated rainfall helps increase the soil moisture and latent heat flux. These features can help establish an increased θ_e in the PBL as well as the large-scale surface flow.

These previous studies revealed that land surface processes contribute to forming favorable condition of convection over the Amazon basin in two different ways. One is a local effect in an increase of θ_e in the lower atmosphere by heat fluxes. Another is indirect. A strong land surface warming forms a large gradient of temperature in the lower atmosphere between land and ocean. This surface temperature gradient thermally drives large-scale circulation that provides moisture into the inland southern Amazon. Although these two effects set a necessary condition for the rapid onset of convection over the Amazon basin, they do not fully explain how the meridional distribution of θ_e in the lower atmosphere is related to the peculiar meridional movement of rain band over the entire South America.

The present study examines how large-scale θ_e in the meridional direction over the South America modulates the seasonal migration of the rain band based on observational data. Our analysis leads to a hypothesis that the equatorial asymmetry in the meridional migration of South American rainfall is closely related to meridional gradients of θ_e, which are affected by the seasonal cold tongue in the equatorial Atlantic Ocean as well as land-sea contrast in heat capacity. We will further examine the influences of the Atlantic cold tongue on θ_e over South America by evaluating atmospheric general circulation model (AGCM) experiments with and without the seasonal modulation of the Atlantic cold tongue.

The rest of the paper is organized as follows. Section 2 describes the datasets and methods employed in the present study. Sections 3 and 4 present the results of our observational analysis and AGCM experiment, respectively. Section 5 is summary and discussion.

2. Method

2.1 Observational analysis

We use the Tropical Rain Measuring Mission (TRMM) satellite monthly accumulated rainfall dataset (3B43 product) from January 1998 to December 2007, available on a 0.25° grid. To examine thermal structures in the lower atmosphere, we also use the monthly Japanese reanalysis datasets (hereafter JRA-25, Onogi et al. 2007), available on 2.5° grid, for the same period as the TRMM rainfall. The variables include temperature, water vapor mixing ratio, geopotential height and wind velocity. Based on these data, monthly climatologies for the 10-year period of 1998–2007 are calculated for the following observational analysis.

2.2 AGCM experiment

To seek key processes involved in the meridional migration of the tropical rain band, we use the AGCM jointly developed at Center for Climate System Research (CCSR) of The University of Tokyo and National Institute for Environmental Studies (NIES). The model resolution is a triangu-

lar truncation at 42 wave numbers (T42) in the horizontal and 20 sigma-levels in the vertical. Realistic continental distribution and topography are given to the model. Standard physical processes such as the modified Arakawa-Schubert cumulus parameterization (Arakawa and Schubert 1974), radiative transfer (Nakajima and Tanaka 1986), and a bucket model for land surface processes (Manabe et al. 1965) are incorporated. Further description is documented in Numaguti et al. (1995), Shen et al. (1998), and Okumura and Xie (2004).

To capture the effect of the Atlantic cold tongue on the rain band over the South American and African continents, we conduct two experiments. One is a control experiment run with the atmospheric model intercomparison project (AMIP I) monthly SST and sea ice (Gates 1992). The other is a "no equatorial annual cycle experiment", with the Atlantic equatorial annual cycle in SST reduced to its annual mean. Both experiments start from a same initial condition. Further details of this experiment are later documented in Section 4. To calculate the climatology in each of the experiments, output for the last 16 out of 20 years is employed.

3. Observational findings

3.1 Rainfall

Figures 1b, 1c contrast the seasonal cycle of rainfall between the all-ocean Atlantic (20–10°W) and all-land African (20–30°E) sectors, based on the TRMM monthly climatology for the 10-year period of 1998–2007. Confined to the north of the equator year round, the rainfall maximum in the Atlantic sector migrates slowly and smoothly between 2–3°N and 10°N, reaching the southernmost and northernmost latitudes in March and August, respectively. The African rain band, on the other hand, displays much larger swings in the meridional direction, with its maximum moving back and forth across the equator between 15°S and 5°N following the sun (the 100 mm month^{-1} contour encompasses a larger latitudinal range of 20°S–15°N). The northern reach of the African rainfall is much smaller than the southern one presumably because of dry land surface conditions in the Sahara desert. In a broad sense, the seasonal cycle of the African rain band is symmetrical between its northward and southward migrations[1], smoothly crossing the equator. The above characteristics of the seasonal migration of tropical rainfall over land and ocean are consistent with Mitchell and Wallace (1992).

The seasonal cycle of rainfall in the South American (60–50°W) sector is very different, highly asymmetric between its northward and southward migrations (Fig. 1a). The rain band moves gradually northward from October to July, shifting the rainfall maximum from 12°S to 10°N across the equator. The equator experiences the maximum rainfall in March–April. This gradual northward migration of rainfall over South America is similar to that over Africa. What happens in and after August is very different between the two continents. From August to October, the marine ITCZ is weak but a large rainfall maximum develops suddenly around 10°S over South America (Fig. 1a), the latter corresponding to the abrupt onset of the South American monsoon (Gan et al. 2004; Zhou and Lau 1998; Horel et al. 1989). On horizontal maps, rainfall is found on the northern edge of South America in August (Fig. 2a) but spreads abruptly southward to 10–20°S in October (Fig. 2b). This South American rainfall maximum continues to intensify and begins moving northward during October–December. North of the equator, there is a secondary rainfall maximum that originates from the marine ITCZ in August, shows a tendency to move southward from August to January, and eventually merges near the equator in January with the northward-migrating major rain band (Fig. 1a). The lack of a gradual southward migration of the major rain band causes an asymmetry between equinoxes: rainfall is at its maximum in March–April but minimum in September–October near the equator. In the Amazon basin south of the equator, rainfall displays a pronounced annual cycle with the rainy season during October to April. Between 5°S and the equator on the African Continent, by contrast, rainfall peaks twice a year associated with the northward and southward migrations of the rain band.

We have examined TRMM rainfall in individual years and the above differences between the African and South American sectors are present every year during 1998–2007 (not shown), characterized by the presence and lack of a gradual southward migration of the major rain band, respectively. The August-to-October abrupt jump in the major rainfall maximum in the South American sector is in-

1 The African rain band also shows a weak asymmetry in its meridional migration, probably related with the West African Monsoon, but the present study focuses on larger asymmetry in the South American sector.

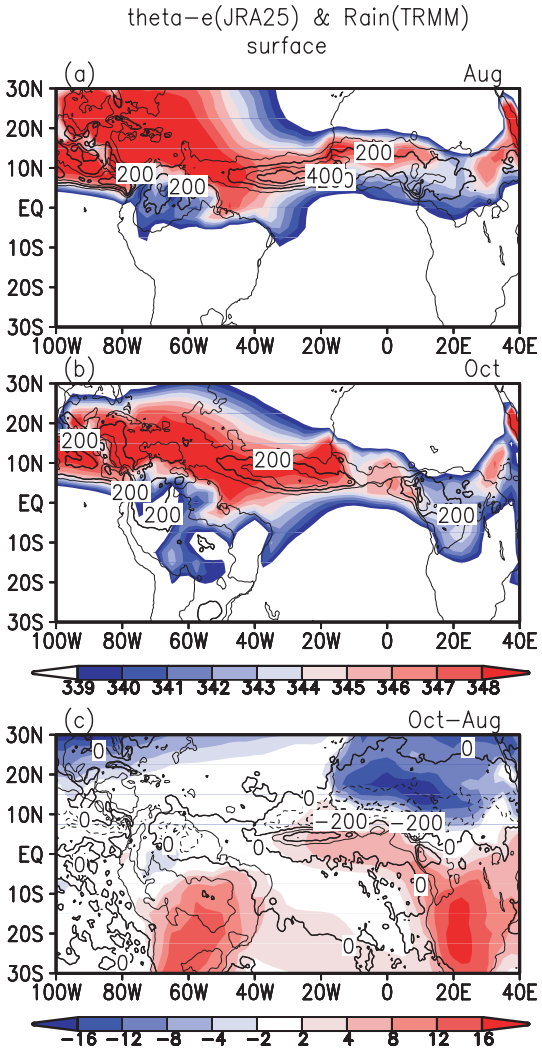

Fig. 2. Equivalent potential temperature (colors in K) at the surface based on the JRA-25 and TRMM rainfall (contours at 100 mm month^{-1} intervals) in (a) August, (b) October, and (c) their differences.

sensitive to the choice of longitudinal span for average and is still present in a wider longitudinal average of 70–40°W band (not shown). The next section examines the factors giving rise to the asymmetry between the northward and southward migrations of the South American rain band.

3.2 *Equivalent potential temperature*

The marine ITCZ over the Atlantic tends to follow the meridional SST maximum with its seasonal march. The continental rain band, however, does not always form over the local maximum of land surface temperature because soil moisture is also a factor. Often increased land surface temperature is a result of lack of rainfall and soil moisture to evaporate water from the ground and balance solar radiation heating. Here we examine equivalent potential temperature (θ_e) at the surface, which is a function of both temperature and humidity and a good measure of atmospheric moist stability. High θ_e favors deep convection. Indeed in Fig. 2, meridional maxima in θ_e derived from the JRA-25 monthly climatology for the 10-year period of 1998–2007 tend to be collocated with rainfall maxima, over both land and ocean.

In Fig. 1, the latitude-time diagrams of θ_e in the American, Atlantic and African sectors are superimposed on TRMM rainfall in contours. In the Atlantic sector with relative humidity around 80%, SST dictates near-surface θ_e. The marine ITCZ tends to follow the meridional maximum of θ_e (Fig. 1b).

In the South American sector, there is an asymmetry between the northward and southward migrations of the θ_e maximum (Fig. 1a). From December to June, there is one single meridional maximum in θ_e and it moves gradually northward together with the rainfall maximum. The situation becomes complicated from July to November, during which the θ_e maximum hardly ever moves southward as the sun does. The northern maximum is associated with the marine ITCZ and has greater values than the southern one until the latter develops in November. The intensification of the southern θ_e maximum is due to the seasonal increase in solar radiation in the Southern Hemisphere and the resultant increase in surface temperature. The southern θ_e maximum eventually exceeds the northern maximum under the marine ITCZ, triggering deep convection that signals the onset of the South American monsoon in November. During this transition period of July–November, the northern θ_e maximum remains nearly constant at 348 K due to large thermal inertia of the ocean. Meanwhile the southern maximum rapidly increases from below 339 to 344 K.

On horizontal maps, maximum θ_e at the surface in August is found near the north coast of South America and the Caribbean Sea, with θ_e decreasing rapidly southward in the Amazon basin (Fig. 2a). While varying little in the tropical ocean and northern South America, θ_e increases rapidly from August to October over the Amazon (Fig. 2b). The October–August difference field (Fig. 2c) shows

that large rainfall increase over the region from the Amazon to the subtropical South America east of the Andes is associated with a local increase in θ_e but there is little change in θ_e near the northern coast of South America and the Caribbean Sea. In October when land convection begins to develop around 10°S, surface θ_e there is still much smaller than over the Caribbean in monthly mean. The diurnal cycle is much larger over land than ocean, likely to play a role in initiating land convection south of the equator in October. Indeed, Kikuchi and Wang (2008) showed a large diurnal variation and an afternoon peak in rainfall over South America. Our analysis of JRA-25 data shows that daytime maximum in land surface θ_e is 6–9 K above the daily mean at 10°S in October. In addition to the daytime increase in land surface θ_e, the daytime PBL is much deeper over land than ocean. Increased θ_e in the well-mixed deep PBL over land leads to an increase in Convective Available Potential Energy (CAPE), which favors October convection over South America around 10°S.

During the South American monsoon from December to June, the θ_e maximum in and south of the continental rain band is well above 344 K (Fig. 1a). The slight poleward displacement of the θ_e maximum relative to the continental rain band may reflect that the interaction between soil moisture and inland-advancing rain band is not in equilibrium due to slow adjustments of ground hydrology. Dry ground limits local moisture supplies for deep convection. The gradual wetting of the ground slows the rain band's inland advance behind the sun's seasonal march (Xie and Saiki 1999).

Near equatorial South America, θ_e remains low below 344 K from July through November, preventing the rain band from migrating southward across the equator (Fig. 1a). Then what maintains low θ_e values near equatorial South America? To answer this question, we need to consider variations in the east-west direction. Figure 3 shows the seasonal cycle of θ_e and wind velocity at 925 hPa meridionally averaged in 5°S–5°N from South America all the way to the African Coast. The 925 hPa level is within the planetary boundary layer from which deep convection originates, and it is above most orography to allow us to see zonal variations of θ_e without the topographic bias. Over the equatorial Atlantic, θ_e reaches an annual minimum in July because of intensified ocean upwelling in response to the increased southeast trades (Mitchell and Wallace 1992; Okumura and Xie 2004). During June–October, θ_e is much lower over the ocean (low in temperature and specific humidity) than over land, and the inland advection by the prevailing easterlies keeps θ_e low over equatorial South America. During February–April, the land-sea θ_e contrast is much relaxed, with ocean upwelling suppressed and θ_e increasing over the equatorial Atlantic. The annual cycles in upwelling cooling and θ_e appear to be a key to the differences between the March and September equinoxes in θ_e over equatorial South America. In March, θ_e is high enough to support deep convection over equatorial South America but it is not in September. The next section examines the effect of the Atlantic cold tongue on the South American rainfall with AGCM experiments.

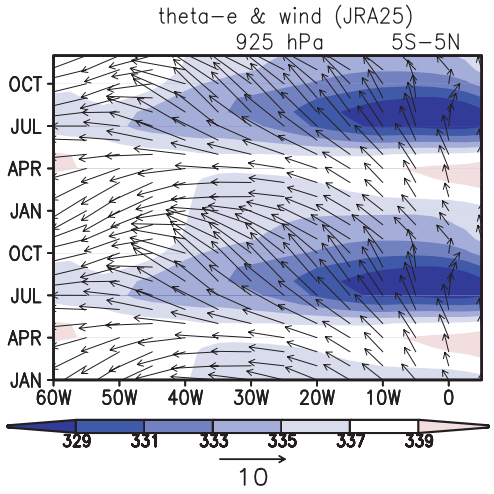

Fig. 3. A longitude-time section of JRA-25 equivalent potential temperature (colors in K) and wind velocity (arrows in m s^{-1}) at 925 hPa averaged over the 5°S–5°N band.

4. AGCM experiment

4.1 Experimental design

The observed annual cycle of tropical Atlantic SST is characterized by the equatorial cold tongue (below 26°C) development east of 25°W during June–October (Fig. 4a). Similar to the SST annual cycle, θ_e at 925-hPa in the ocean east of 40°W shows the cooling in the cold tongue season (Fig. 3). We conduct the control AGCM simulation (CTRL) with prescribed monthly climatological SST. We then conduct an AGCM experiment forced by the same SST outside of the tropical Atlantic but with no equatorial annual cycle (NEAC) in the Atlantic. Specifically, we apply a meridional

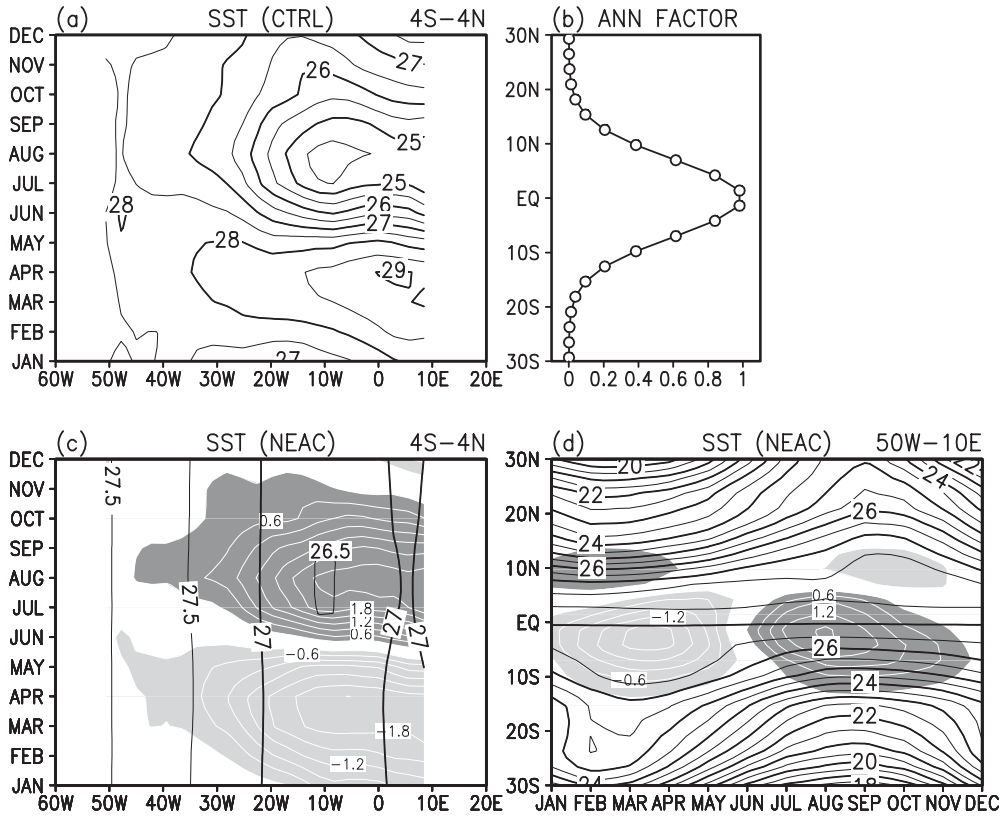

Fig. 4. (a) A longitude-time section of the climatological annual cycle in AMIP SST (contours at 0.5°C intervals) in the equatorial Atlantic (4°N–4°S) as the prescribed SST field for the CTRL run. (b) A latitudinal plot of the annual mean factor applied to the tropical Atlantic SST. This factor is applied for the No-Equatorial-Annual-Cycle. (c) As in (a), but for the NEAC SST (contours at 0.5°C intervals). Shades with white contours at 0.3°C intervals are differences of SST between the CTRL and the NEAC experiments. (d) As in (c), but for a latitude-time section zonally averaged for 50°W–10°E.

weight function (Fig. 4b) to tropical Atlantic SST in order to reduce the equatorial annual cycle. The weight function, $\alpha(y)$, is set as below:

$$\alpha(y) = \exp[-(y/10)^2], -30 < y < 30,$$

where y is a latitude in degree. The SST for the NEAC experiment, Ts_{NEAC}, is set as below:

$$Ts_{\mathrm{NEAC}}(t) = [1 - \alpha(y)]Ts_{\mathrm{CTRL}}(t) + \alpha(y)\overline{Ts_{\mathrm{CTRL}}},$$

where $Ts_{\mathrm{CTRL}}(t)$ is the AMIP I monthly climatology of SST for the CTRL experiment and $\overline{Ts_{\mathrm{CTRL}}}$ is the annual mean of $Ts_{\mathrm{CTRL}}(t)$. For example, $Ts_{\mathrm{NEAC}}(t) = \overline{Ts_{\mathrm{CTRL}}}$ at the equator where $\alpha(y) = 1$, and $Ts_{\mathrm{NEAC}}(t) = Ts_{\mathrm{CTRL}}(t)$ in the mid- and higher latitudes where $\alpha(y) = 0$. With this modified SST field in the tropical Atlantic, the annual cycle is strongly reduced in the equatorial Atlantic (4°S–4°N, Figs. 4c and 4d) but remains largely unchanged poleward of 10°N/S on either side of the equator (Fig. 4d). To see the cold tongue's influence on θ_e and rainfall in September equinox near equatorial South America, we examine the difference between the CTRL and NEAC experiments. Both experiments start from the same, isothermal, and static initial condition, and the last 16-year results out of 20-year runs are analyzed for model climatology.

4.2 *Effect of Atlantic cold tongue on Amazon rainfall*

The CTRL experiment successfully reproduces the observed meridional migration of the tropical rain band in South America, Atlantic, and African sectors. Over equatorial South America (Fig. 5a), the simulated rainfall maximum is located over high surface θ_e (354 K$\sim$) in March equinox and its minimum over low surface θ_e ($\sim$344 K) in Sep-

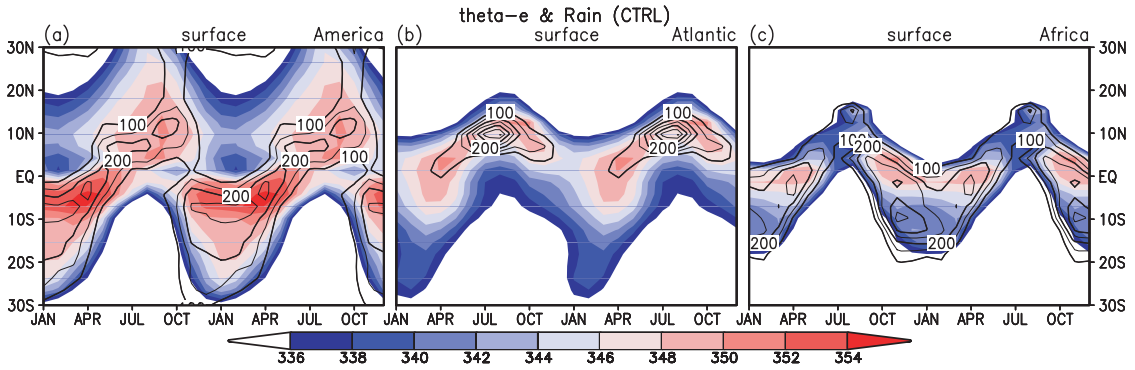

Fig. 5. Latitude-time sections of simulated (CTRL experiment) equivalent potential temperature at the surface (colors in K) averaged over the (a) South American (60–50°W), (b) Atlantic (20–10°W), and (c) African (20–30°E) sectors. Superimposed are of the 100, 150, 200 and 250 mm month^{-1} contours for rainfall.

tember equinox. As a result, the annual cycle—strong northward and weak southward movements of the rain band and surface θ_e in particular—is well reproduced in the CTRL simulation.

The year-round, northward displacement of the rain band over the tropical Atlantic (Fig. 5b) is well simulated in the CTRL. The African rain band in the CTRL is of comparable intensities for the northward and southward movements through the annual cycle as observed (Figs. 1c, 5c), while the rainfall maximum during austral summer (November–January) in 5–15°S is 2–3 times larger than in TRMM observations. These rain bands mostly follow the local maximum of surface θ_e, but surface θ_e values over the land in the CTRL tend to be higher by 2–6 K than in the JRA-25, probably due to an unrealistic representation of soil moisture in a bucket model. High surface θ_e destabilizes the atmosphere and causes excessive rainfall.

In the NEAC experiment, the rain bands over the Atlantic and African sectors mostly retain their characteristic features as mentioned in the CTRL experiment, albeit with slightly enhanced local maximum (Figs. 6b, c). The only major difference over the Atlantic sector is the reduced seasonal cycle of surface θ_e due to suppressed SST variations (Figs. 6b, e). As a result, the maximum in March–April over the equator is much reduced (Figs. 6b, e). The reduced annual cycle over the Atlantic causes no major difference in the rain band over African between the experiments (Figs. 6c, f). These results show that the Atlantic cold tongue's influence does not extend far eastward.

By contrast, the meridional migration of the South American rain band in the NEAC experiment is very different from that in the CTRL experiment. Although SST modification is limited to the equatorial Atlantic, the annual cycle in surface θ_e nevertheless weakens in NEAC over equatorial South America (Figs. 6a, d). This illustrates a strong influence of equatorial Atlantic SST on the annual cycle in surface θ_e over equatorial South America, probably due to the advection by the mean easterly trades. Specifically, surface θ_e in March–May (September–November) over equatorial South America in the NEAC experiment is lower (higher) by 3 K, than in the CTRL (Fig. 6d), comparable in magnitude to surface θ_e difference over the equatorial Atlantic between the experiments (Fig. 6e). The maximum (minimum) in surface θ_e differences in the March (September) equinox leads to an increase (decrease) in rainfall by 50–75 mm month^{-1} (Fig. 6d). In the NEAC experiment, these changes enhance (weaken) discontinuity in the South American rain band in the March (September) equinox. As a result, the South American rain band encompassed by 100 mm month^{-1} contours in Fig. 6a is not so substantially different between the northward and southward migrations. Rainfall in 5–12°N decreased (increased) in March–May (August–September) in the NEAC experiment, compared to the CTRL experiment (Fig. 6d). This off-equatorial difference in rainfall is not fully associated with changes in local surface θ_e. Therefore, correlation between θ_e and rainfall is weaker in Fig. 6a than in Fig. 5a, particularly in the Northern Hemisphere. The changes in equato-

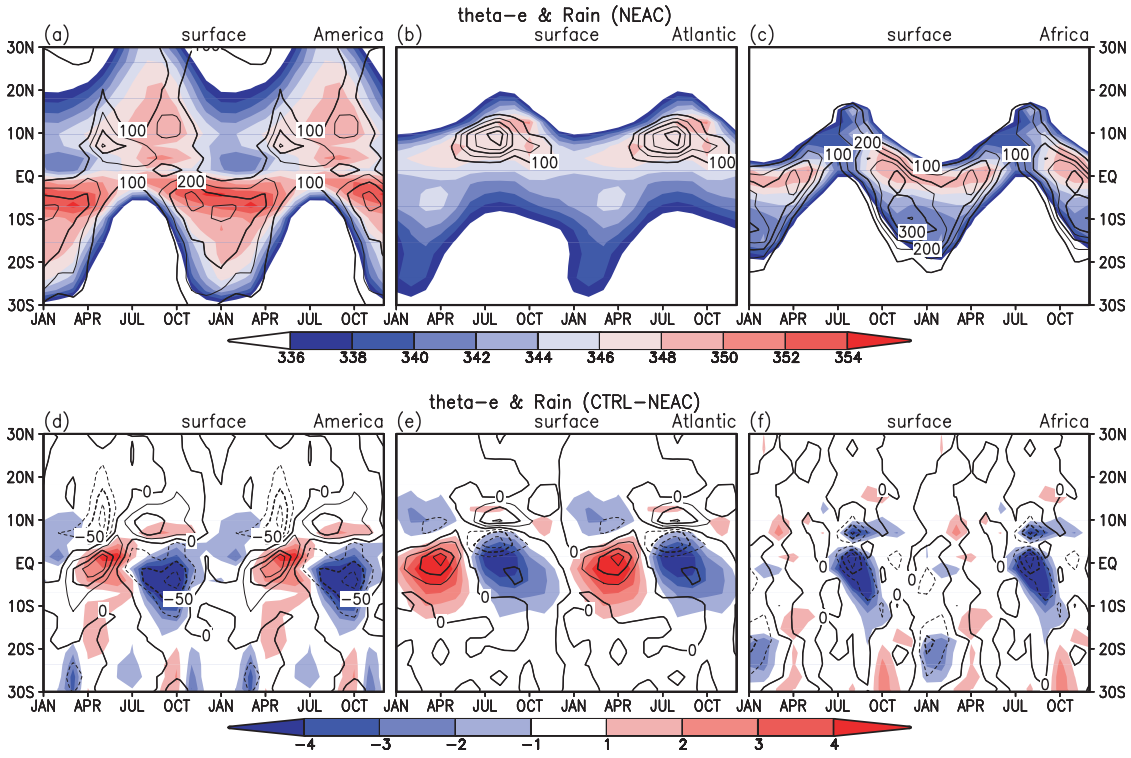

Fig. 6. (a–c) As in Fig. 5, but for the NEAC experiment. (d–f) As in (a–c), but for the difference of equivalent potential temperature at the surface (colors in K) and rainfall (contours at 25 mm month^{-1} intervals).

rial conditions can modify the strength of the local Hadley circulation and bring about remote impacts on the off-equatorial rainfall. Gan et al. (2004) showed the influence of the local Hadley circulation on the rainy season onset over western-central Brazil.

Very low values of surface θ_e (< 344 K) over equatorial South America in September–October are found in the CTRL but not in the NEAC experiment, while a local maximum of surface θ_e over the Caribbean Sea (5–20°N) for the same period is found in both experiments. These results suggest that large thermal inertia over the Caribbean Sea is not directly responsible for the local minimum of surface θ_e and resultant dry spell over the Amazon in the September equinox. Rather, the Atlantic cold tongue is a source of low surface θ_e, which affects equatorial South America in September–October via advection. Figure 7 displays the difference fields in the surface θ_e, wind velocity and rainfall averaged in 5°S–5°N between the CTRL and NEAC experiments. The cold tongue in the far eastern Atlantic begins to form in July with the onset of the

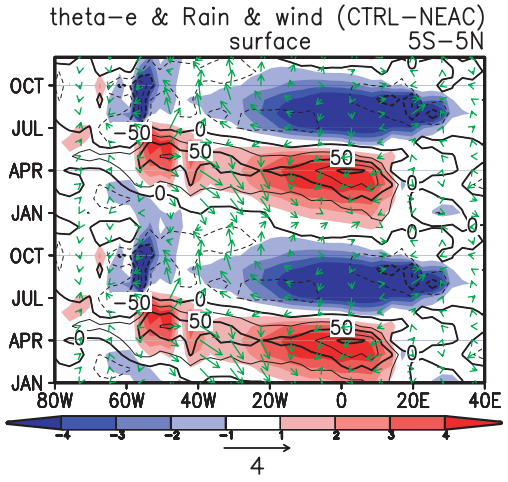

Fig. 7. A longitude-time section of differences equivalent potential temperature (colors in K), wind velocity (arrows in m s^{-1}) and rainfall (contours at 25 mm month^{-1} intervals) at the surface averaged latitudinally for 5°S–5°N between the CTRL and the NEAC experiments.

African Monsoon and propagates westward by air-sea interaction (Okumura and Xie 2004). The thermal advection by the mean easterly trade begins to form anomalous low θ_e at the surface in August over 45–65°W, affecting the annual cycle of South American rainfall. This negative difference in the surface θ_e remains until the following February. Intense solar radiation in the March equinox increases surface θ_e and destabilizes the overlying atmosphere, initiating the wet spell over the Amazon. In April–July, the thermal advection from the Atlantic helps increase surface θ_e over equatorial South America (Fig. 7), giving rise to a discontinuity in the northward migration of the rain band in the NEAC experiment (Fig. 6a).

Fu et al. (2001) drew a similar conclusion that seasonal variations in tropical Atlantic SST are the key to the dry season of eastern equatorial Amazon at the September equinox, but they based the conclusion on different experiments that allow the SST seasonal cycle over the broad tropical Atlantic between 30°S and 30°N, and set SST elsewhere at the annual mean values. Our experimental design enables the isolation of the seasonal development of the equatorial cold tongue as the cause of suppressed Amazon convection during September–October.

5. Summary and discussion

We have examined the seasonal migration of rainfall in the South American, Atlantic and African sectors. While the African rain band moves gradually both north- and southward following the seasonal march of the sun, the South American rain band displays a unique asymmetry between the north- and southward transitions. While its northward migration is a gradual process as over Africa, the South American convection center jumps abruptly southward from August to October, signaling the onset of the South American monsoon. Over both land and ocean, atmospheric convection centers are found over regions of large equivalent potential temperature (θ_e) at the surface. During July to October, the surface θ_e over equatorial South America is kept low by the easterly advection of low θ_e air cooled by intense ocean upwelling over the equatorial Atlantic. This low θ_e over the equatorial Amazon appears to be critical to preventing deep convection from migrating from the Atlantic ITCZ southward across the equator. Meanwhile, the continuing increase in solar radiation south of the equator keeps raising ground temperature and θ_e, eventually triggering deep convection around 10°S in October.

To identify the effect of ocean upwelling on the South American rain band, we conducted a pair of AGCM experiments with and without the annual cycle in equatorial Atlantic SST. The results support the hypothesis that the advection of low surface θ_e from the equatorial Atlantic by mean easterly trades causes the dry spells during September–October in the equatorial Amazon in the CTRL simulation. There may be interactions between equatorial Amazon rainfall and the Atlantic cold tongue. The present study shows influences of the cold tongue on South American rainfall during the equatorial cold season, and recent analyses of coupled model simulations indicate that Amazon rainfall during the warm season (March–May) affects the subsequent development of the equatorial cold tongue (Chang et al. 2007; Richter and Xie 2008).

Factors other than equatorial SST may also contribute to, such as the land-sea contrast in heat capacity. The role of thermal contrast between South America and the Caribbean/North Atlantic needs to be further explored. Let us compare March and September equinoxes. In March, the South American rain band is located near the equator and in no hurry to jump northward as Caribbean and North Atlantic SST to the north is still cool. As a result, the northward migration of rainfall can be gradual and slow. In September, by contrast, Caribbean and North Atlantic SST is at its annual maximum preventing convection from taking place pre-maturely over the continent to the south and allowing θ_e to build up for an abrupt onset of land convection over South America. This may contribute to the abrupt onset of land convection over South America, aided by cold air intrusions from the extratropics (Garreaud and Wallace 1998; Li and Fu 2006). While our focus is on the climatological annual cycle, Grimm et al. (2007) and Grimm and Zilli (2009) showed, in the context of interannual variability, that previous conditions in austral spring in terms of soil moisture and near surface temperature may influence the peak monsoon rainfall over South America.

Acknowledgments

The authors wish to thank Drs. H. Matsuyama, M. Watanabe, F. Hasebe, K. Yamazaki, and H. Hatsushika for useful discussion, and CCSR/NIES model developers for the model code. Model ex-

periments were performed on IPRC SGI servers and JAMSTEC NEC SX-8R. This work was supported in part by the Global Environment Research Fund (S-5) of the Ministry of the Environment, Japan, Grand-In-Aid for Scientific Research defrayed by the Ministry of Education, Culture, Sports, Science and Technology of Japan (18204044), NOAA, NASA, and JAMSTEC. This is IPRC publication 655 and SOEST publication 7850.

References

Arakawa, A., and W. H. Schubert, 1974: Interactions of cumulus cloud ensemble with large-scale environment. *J. Atmos. Sci.*, **31**, 671–701.

Chang, C. Y., J. A. Carton, S. A. Grodsky, and S. Nigam, 2007: Seasonal Climate of the Tropical Atlantic Sector in the NCAR Community Climate System Model 3: Error Structure and Probable Causes of Errors. *J. Climate*, **20**, 1053–1070.

Fu, R., B. Zhu, and R. E. Dickinson, 1999: How do atmosphere and land surface influence seasonal changes of convection in the tropical Amazon? *J. Climate*, **12**, 1306–1321.

Fu, R., R. E. Dickinson, M. Chen, and H. Wang, 2001: How do tropical sea surface temperatures influence the seasonal distribution of precipitation in the equatorial Amazon? *J. Climate*, **14**, 4003–4026.

Fu, R., and W. Li, 2004: The influence of the land surface on the transition from dry to wet season in Amazonia. *Theor. Appl. Climatol.*, **78**, 97–110.

Gan, M. A., V. E. Kousky, and C. F. Ropelewski, 2004: The South America monsoon circulation and its relationship to rainfall over west-central Brazil. *J. Climate*, **17**, 47–66.

Garreaud, R. D., and J. M. Wallace, 1998: Summertime incursions of midlatitude air into subtropical and tropical South America. *Mon. Wea. Rev.*, **126**, 2713–2733.

Gates, W. L., 1992: AMIP, The Atmospheric Model Intercomparison Project. *Bull. Amer. Meteor. Soc.*, **73**, 1962–1970.

Grimm, A. M., J. Pal, and F. Giorgi, 2007: Connection between spring conditions and peak summer monsoon rainfall in South America: Role of soil moisture, surface temperature, and topography in eastern Brazil. *J. Climate*, **20**, 5929–5945.

Grimm, A. M., and M. T. Zilli, 2009: Interannual variability and seasonal evolution of summer monsoon rainfall in South America. *J. Climate*, **22**, 2257–2275.

Horel, J. D., A. N. Hahmann, and J. E. Geisler, 1989: An investigation of the annual cycle of convective activity over the tropical Americas. *J. Climate*, **2**, 1388–1403.

Kikuchi, K., and B. Wang, 2008: Diurnal precipitation regimes in the global tropics. *J. Climate*, **21**, 2680–2696.

Kodama, Y.-M., 1992: Large-scale common features of subtropical precipitation zones (the Baiu frontal zone, the SPCZ and the SACZ) Part I: Characteristics of subtropical frontal zones. *J. Meteor. Soc. Japan*, **70**, 813–836.

Kodama, Y.-M., 1993: Large-scale common features of subtropical convergence zones (the Baiu frontal zone, the SPCZ and the SACZ) Part II: Conditions of the circulations for generating the STCZs. *J. Meteor. Soc. Japan*, **71**, 581–610.

Kodama, Y.-M., and A. Tamaoki, 2002: A reexamination of precipitation activity in the subtropics and the mid-latitudes based on satellite-derived data. *J. Meteor. Soc. Japan*, **80**, 1261–1278.

Li, W., and R. Fu, 2004: Transition of the large-scale atmospheric and land surface conditions from the dry to the wet season over Amazonia as diagnosed by the ECMWF Re-Analysis. *J. Climate*, **17**, 2637–2651.

Li, W., and R. Fu, 2006: Influence of Cold Air Intrusions on the Wet Season Onset over Amazonia. *J. Climate*, **15**, 257–275.

Lietzke, C. E., C. Deser, and T. H. Vonder Haar, 2001: Evolutionary structure of the Eastern Pacific double ITCZ based on satellite moisture profile retrievals. *J. Climate*, **14**, 743–751.

Manabe, S., J. Smagorinski, and R. F. Strickler, 1965: Simulated climatology of a general circulation model with a hydrologic cycle. *Mon. Wea. Rev.*, **93**, 769–798.

Marengo, J. A., B. Liebmann, V. E. Kousky, N. P. Filizola, and I. C. Wainer, 2001: Onset and end of the rainy season in the Brazilian Amazon Basin. *J. Climate*, **14**, 833–852.

Mitchell, T. P., and J. M. Wallace, 1992: The annual cycle in equatorial convection and sea surface temperature. *J. Climate*, **5**, 1140–1156.

Nakajima, T., and M. Tanaka, 1986: Matrix formulation for the transfer of solar radiation in a plane-parallel scattering atmosphere, *J. Quant. Spectrosc. Radiat. Transfer*, **35**, 13–21.

Numaguti, A., M. Takahashi, T. Nakajima, and A. Sumi, 1995: Description of CCSR/NIES atmospheric general circulation model. In Climate System Dynamics and Modeling, T. Matsuno, Ed., CCSR/Univ. of Tokyo.

Okumura, Y., and S.-P. Xie, 2004: Interaction of the Atlantic equatorial cold tongue and the African Monsoon. *J. Climate*, **17**, 3589–3602.

Onogi, K., et al., 2007: The JRA-25 Reanalysis. *J. Meteor. Soc. Japan*, **85**, 369–432.

Raia, A., and I. F. d.A. Cavalcanti, 2008: The life cycle of the South American monsoon system. *J. Climate*, **21**, 6227–6246.

Richter, I., and S.-P. Xie, 2008: On the origin of equatorial Atlantic biases in coupled general circulation models. *Clim. Dyn.*, **31**, 587–598.

Shen, X., M. Kimoto, and A. Sumi, 1998: Role of land surface processes associated with interannual variability of broad-scale Asian summer monsoon as simulated by the CCSR/NIES AGCM. *J. Meteor. Soc. Japan*, **76**, 217–236.

Waliser, D. E., and C. Gautier, 1993: A satellite-derived climatology of the ITCZ. *J. Climate*, **6**, 2162–2174.

Wang, H., and R. Fu, 2002: Cross-equatorial flow and seasonal cycle of precipitation over South America. *J. Climate*, **15**, 1591–1608.

Williams, E., and N. Renno, 1993: An analysis of the conditional instability of the tropical atmosphere. *Mon. Wea. Rev.*, **121**, 21–36.

Xie, S.-P., and S. G. H. Philander, 1994: A coupled ocean-atmosphere model of relevance to the ITCZ in the eastern Pacific. *Tellus*, **46A**, 340–350.

Xie, S.-P., and N. Saiki, 1999: Abrupt onset and slow seasonal evolution of summer monsoon in an idealized GCM simulation. *J. Meteor. Soc. Japan*, **77**, 949–968.

Zhou, J., and K.-M. Lau, 1998: Does a monsoon climate exist over South America? *J. Climate*, **11**, 1020–1040.